Article submitted to: High Power Laser Science and Engineering, 2025 *February 20, 2025*

Assistance of Four-Wave Mixing for the Achievement of 4kW Raman fiber amplifier

Chenchen Fan[1], Tianfu Yao[1,2,3], Xiulu Hao[1], Yang Li[1], Jinyong Leng[1,2,3], and Pu Zhou[1]

[1]*College of Advanced Interdisciplinary Studies, National University of Defense Technology, Changsha 410073, China.*
[2]*Nanhu Laser Laboratory, National University of Defense Technology, Changsha 410073, China.*
[3]*Hunan Provincial Key Laboratory of High Energy Laser Technology, Changsha 410073, China.*

Abstract
Raman fiber lasers, known for their capacity to provide both high-power and precise wavelength emissions, are gaining attraction across a spectrum of applications, including fiber optic communications, sensing, spectroscopy, and imaging. However, the scalability of Raman laser power is impeded by the constraints of pump brightness and the deleterious effects of second-order Raman scattering. In this research, we have undertaken a comprehensive experimental and simulation-based investigation into the impact of pump brightness on the output characteristics within an amplifier framework. Our innovative approach integrates high-brightness pumping with multi-mode graded index fibers. Notably, we have pioneered the introduction of multi-wavelength seed light to facilitate four-wave mixing, thereby effectively mitigating higher-order Raman scattering. This novel strategy has culminated in the achievement of a 4 kW Raman laser output in an all-fiber configuration, representing the highest output power reported so far.

Keywords: fiber laser; stimulated Raman scattering; graded-index fiber; Raman amplifier

1. Introduction

Fiber lasers, known for their superior beam quality, high efficiency, compact design, and effective heat dissipation, have been widely adopted in various fields[1–3] such as industrial processing[4,5], medical applications[6,7], telecommunications[8,9], and scientific research[10,11]. The swift evolution of semiconductor lasers, fiber optics, and fiber devices has catalyzed remarkable advancements in the development and deployment of high-power fiber lasers. Notably, rare-earth-ion-doped fiber lasers[12,13], exemplified by ytterbium-doped varieties[14–16], have risen to prominence in research circles due to their prowess in delivering high-power outputs, with these lasers now attaining tens of kilowatt output capabilities. However, these lasers are inherently limited to achieving high-power output within a narrow wavelength spectrum because of the specific energy-level radiation characteristics of rare-earth ions. Raman fiber lasers, taking advantage of the stimulated Raman scattering (SRS) effect, present a compelling alternative[17,18]. They offer an expansive gain bandwidth and capacity for cascade operation, facilitating a broad spectrum of Raman frequency shifts. By strategically selecting an appropriate pump source, it is theoretically feasible to achieve lasers across any wavelength supported by the fiber, rendering Raman fiber lasers an optimal solution for combining arbitrary wavelength flexibility with high-power capabilities[19–24].

Raman oscillators, particularly those based on fiber Bragg gratings, have reaped the benefits of advancements in fiber technology, boasting a simple structure and achieving power outputs that span from hundreds of watts to several kilowatts. Initially, Raman fiber lasers were primarily based on small-core step-index fibers, a structure that limited the injection power of pump light and, due to the high-power density of signal light within the core, resulted in a lower threshold for second-order Raman light. This restricted further increase in laser power, with the maximum output power mostly remaining in the 100-watt level[25,26]. With the application of cladding pumping schemes in Raman fiber oscillators, the injectable pump power was effectively increased, enabling the output power of Raman fiber oscillators to jump from the hundred watt[27] to several hundred watts[28] or even the kilowatt range[29]. However, cladding pumping schemes require

Correspondence to: Tianfu Yao and Pu Zhou, College of Advanced Interdisciplinary Studies, National University of Defense Technology, Changsha 410073, China. Email: yaotianfumary@163.com (T. Yao), zhoupu203@163.com (P. Zhou)

10.1017/hpl.2025.29
https://doi.org/10.1017/hpl.2025.29 Published online by Cambridge University Press

special fiber design, and the stimulated Raman scattering of pump light in the cladding may lead to a decline in laser output quality. In contrast, the core pumping scheme based on large-core multimodal graded-index fibers not only enhances the injectable pump power but also achieves high-power, high-beam-quality Raman fiber laser output through various brightness enhancement mechanisms such as beam purification and resonant cavity mode selection. Currently, the maximum output power of Raman oscillators based on multimodal fiber core pumping has evolved from the hundred-watts to the kilowatt level [30–33], with the current record reaching 1780W [34].

On the other hand, Raman amplifiers, despite their increased structural complexity, possess a clear advantage when it comes to achieving high-power outputs. Utilizing specialized fiber designs, high-power pump sources, and sophisticated fiber devices, these lasers have successively achieved output powers of hundreds watts [19,35]. By continuously optimizing fiber devices such as couplers and employing multimode fibers with larger core diameters, the output power has rapidly escalated to the kilowatt level [36,37]. With the enhancement of metal coating technology, the radial heat conduction capability of Raman fibers has been significantly improved. This effective cooling of the Raman fibers at high power levels has led to a further increase in the output power of the laser. The current maximum output power has reached 3000W [38]. While Raman fiber lasers have seen rapid development, their power enhancement is primarily constrained by the emergence and rapid growth of second-order Raman scattering. This scattering not only leads to a decrease in laser efficiency but can also result in thermal damage and nonlinear effects within the laser, impacting its stability and output power. Existing methods to suppress higher-order Raman scattering include using fibers with larger mode field areas and shorter lengths [38], employing cladding pumping with special optimization of the core-to-cladding ratio [29], and optimizing the pump structure in amplifiers to use pump light with better temporal stability [39]. Additionally, designing seed light power and mode characteristics is also an effective method to suppress second-order Raman [40]. However, these methods all have certain limitations, such as high costs, complexity, and low efficiency. Therefore, there is an urgent need to explore further high-order Raman suppression schemes to achieve higher power output in Raman fiber lasers.

In this paper, we investigate the impact of pump brightness on laser output characteristics and validate a feasible scheme for achieving high-power output using high-brightness pumping combined with large-core graded-index fibers. Building on this, we propose a new scheme to suppress higher-order Raman. By utilizing dual-wavelength seed lasers to induce four-wave mixing, new frequency light components are generated in the fiber amplifier, causing the second-order Raman light to interact with the new frequency light components. This interaction transfers part of the optical power to the new frequency components, thereby suppressing the growth of second-order Raman power. Ultimately, we have achieved 4kW Raman fiber amplifier in an all-fiber structure, representing the highest output power of Raman fiber lasers to date. This research not only provides new technical avenues for the development of high-power Raman fiber lasers but also expands the possibilities for further applications of fiber lasers.

2. Experimental setup

To achieve high-power Raman laser output, we have built an all-fiberized Raman amplifier as depicted in Figure 1. The seed light is a Yb-doped oscillator with a central wavelength of 1130nm. The pump light is provided by four high-power Yb-doped oscillators with a central wavelength of 1080nm. The pump light is injected into the amplifier through a home-made (6+1)*1 signal/pump combiner, with a maximum combined pump power of over 5kW. The input fibers of the combiner for both the signal and pump have a same core/cladding diameter of 20/130μm, and the output pigtail is connected to a section of Raman gain fiber with a graded refractive index distribution. Considering our previous research, it has been observed that large-core multimode fibers with a core diameter exceeding 100μm can also achieve near-single-mode output [39]. This is primarily due to the inherent beam-cleaning capability [41] of graded refractive index fibers and the higher gain of stimulated Raman scattering for lower-order modes [42]. In high-power Raman lasers based on large-core fibers, further power enhancement is mainly limited by the emergence and rapid growth of higher-order Raman scattering. To effectively suppress higher-order Raman scattering while maintaining the quality of the output beam, we have specially designed the Raman gain fiber. We have increased the core diameter while appropriately reducing the numerical aperture (NA) of the core. This fiber has a core/cladding diameter of 150/210μm and the NA of the core is 0.25. The refractive index distribution, as shown in the inset of Figure 1, exhibits a parabolic profile. The inherent beam cleaning provided by this graded refractive index distribution is an important guarantee for achieving high-brightness signal light output. To protect the system from the adverse effects of back reflections generated within the amplifier, we have spliced an end cap with an anti-reflective coating that spans the 900-1200nm range at the output end. This design helps to protect the system from the effects of back reflections, ensuring the stability and safety of the system.

3. The impact of pump brightness on laser output

In the amplifier structure, pump light serves as the primary power source for Raman conversion, and its optical characteristics significantly influence the output signal light.

https://doi.org/10.1017/hpl.2025.29 Published online by Cambridge University Press

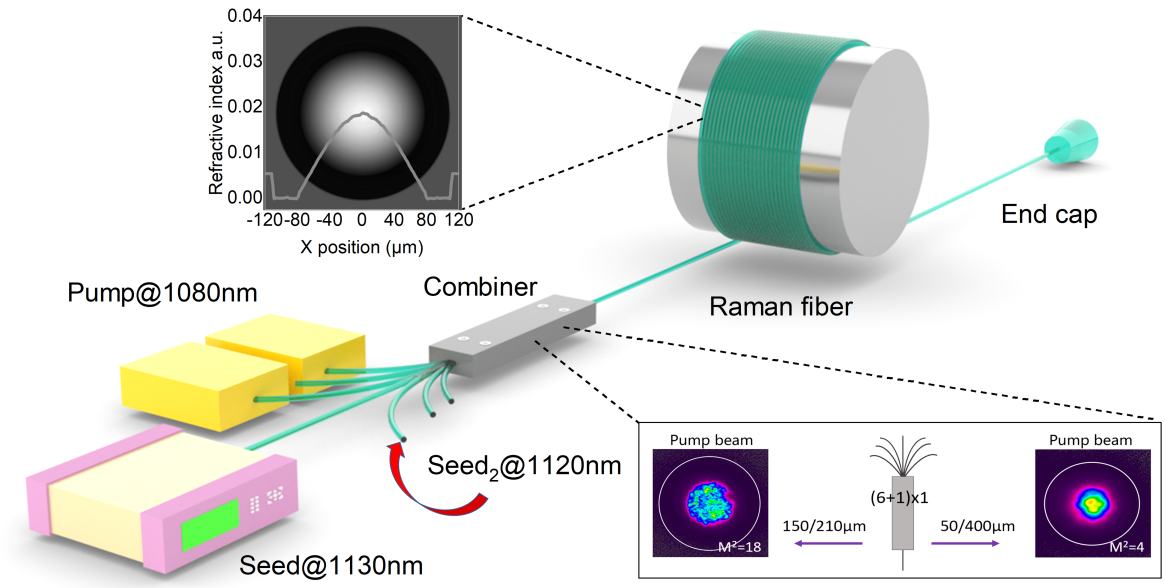

Figure 1. Experimental setup of Raman fiber amplifier. The inset in the top shows the refractive index distribution and the illustration at the bottom of the figure shows the output beam profiles of the pump light after coupling through combiners with different output fiber

Specifically, pump sources with broader spectral linewidths and better temporal stability tend to markedly enhance the output performance of the signal light. Detailed findings of these studies can be found in the literature[43]. The brightness of the pump light also plays a crucial role in the Raman threshold, conversion efficiency, and output power of the laser. To further investigate the influence of pump brightness on the output characteristics of the laser, we employed fiber combiners with different output tail fiber diameters to inject pump light. Specifically, we compared fiber combiners with output tail fibers of 150/210μm (with a core NA of 0.25) and 50/400μm (with a core NA of 0.1). The output beam profiles of the 1080nm pump light after coupling through these combiners are shown in the inset of Figure 1. When the pump light passes through the combiner with a 150μm core, the output fiber has a large core diameter and NA, resulting in a huge number of high-order modes within the fiber. Consequently, the pump light brightness at the output end of the combiner is quite low, leading to a diffuse near-field beam profile distribution. In contrast, after passing through the 50/400μm combiner, the pump light exhibits higher brightness and better beam quality. The near-field pump light spot intensity distribution at the output end of the combiner is illustrated on the right, showing a more concentrated energy distribution.

3.1. Raman fiber amplifier under low-brightness pumping

Initially, the fiber combiner with a large core diameter of 150μm, which has lower brightness, was used for pump injection and the output power and spectrum were measured. The seed light is provided by an ytterbium-doped fiber laser with a central wavelength of 1130 nm and an output power of 130 W. Concurrently, we optimized the length of the fiber within the amplifier by progressively shortening the fiber length. To better investigate the impact of fiber length and pump light brightness on the laser's output characteristics, we defined the maximum output power of the laser under a specific configuration as the point where the intensity of the second-order Raman spectral peak reaches to -40dB relative to the signal light. Due to the further increase of second-order Raman light will reduce the power of the signal light, and additionally, the backward transmission of second-order Raman light can affect the stability of the preceding system.

Figure 2 illustrates the maximum output power achievable by the Raman amplifier at various fiber lengths, along with the corresponding output spectra at maximum power. At a fiber length of 90m, the maximum pump power that can be injected is 2520W, resulting in a total laser output power of 2434W. This includes a signal power of 680W and a remaining pump power of 1754W, corresponding to a Raman conversion efficiency of 26.9%. As the length of the Raman fiber decreases, the threshold for first-order stimulated Raman scattering increases, necessitating higher pump powers for Raman conversion. As depicted in Figure 2(b), a reduction in fiber length leads to a significant increase in the injectable pump power, which in turn causes a continuous growth in the total laser output power. However,

https://doi.org/10.1017/hpl.2025.29 Published online by Cambridge University Press

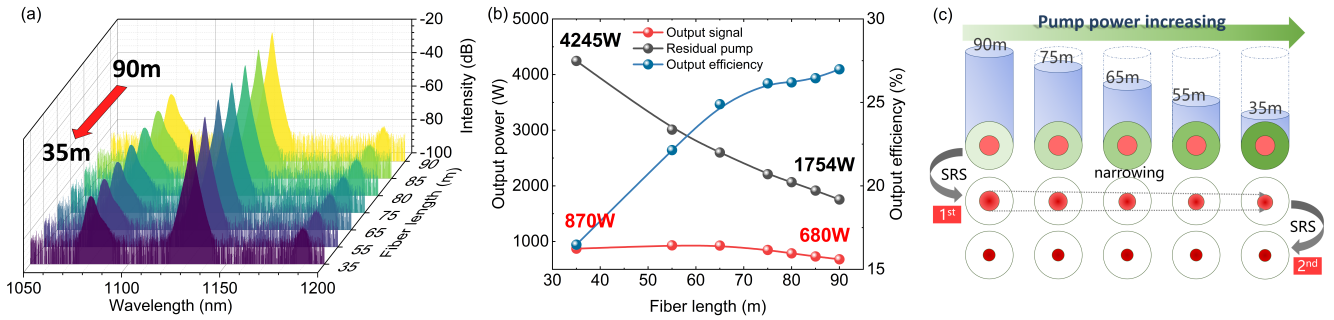

Figure 2. The maximum achievable output power at different fiber lengths with corresponding output spectrum of the Raman fiber amplifier pumped by lower brightness laser. (a) Output spectra power under maximum power at various fiber length; (b) The evolution of output power and efficiency;(c) the physical process behind the constant second-order Raman threshold under low-brightness pumping.

the laser's output efficiency significantly decreases. When the fiber length is reduced to 35m, the maximum injectable pump power reaches 5280W, and the maximum output power of the laser is 5115W. The signal power is 870W, and the remaining pump power is 4245W, corresponding to a Raman conversion efficiency of only 16.5%. The results clearly indicates that when using a low-brightness pump source, the laser's efficiency is low, and it further decreases with the reduction of fiber length. Moreover, the maximum achievable signal power consistently remains at the 800W level, at which point the power is further limited by second-order Raman scattering.

Figure 2(c) demonstrates the physical process behind the constant second-order Raman threshold under low-brightness pumping. Since the response of the stimulated Raman scattering process is related to the peak power of the beam, we assume that the pump light has a nearly Gaussian intensity distribution within the core, being stronger in the center and weaker around the edges. Therefore, as the pump power increases, the higher-intensity pump light closer to the fiber core will reach the stimulated Raman scattering threshold first, undergoing frequency conversion. With the reduction in fiber length, the increased injected pump power means that the same output signal light power at the output end implies that more energy from the pump light closer to the core region has achieved stimulated Raman conversion first. In other words, in shorter fibers, the signal light is converted from the higher-brightness pump closer to the core, resulting in a relatively stronger signal light brightness. The higher brightness of the signal light at the same power compensates for the reduction in second-order Raman scattering due to the shorter fiber. Thus, when the fiber length is shortened, the threshold of second-order Raman scattering exhibits a phenomenon of not changing with fiber length. The main reason for this result is that the fiber core diameter is too large, and the pump brightness in the regions far from the center is too low to reach the stimulated Raman scattering threshold and cannot achieve frequency conversion through stimulated Raman scattering. Therefore, we attempted to use combiner with smaller output fiber core diameters and NA to provide higher-brightness pump light.

3.2. Raman fiber amplifier under high-brightness pumping

Subsequently, the fiber combiner with a smaller core diameter of 50μm, which has higher brightness, was used for pump injection. We further optimized the fiber system by incrementally reducing the fiber length while maintaining a constant intensity for the second-order Raman light. The maximum achievable output power at different fiber lengths with corresponding output spectrum of the Raman fiber amplifier pumped by lower brightness laser was shown in Figure 3. With an initial fiber length of 25m, the maximum pump power we could inject was 1800W. The seed light of 130W, amplified through stimulated Raman scattering within the fiber, resulted in a signal power output of 1060W, with a remaining pump power of 616W, achieving a Raman conversion efficiency of 58.8%. As the fiber length decreased, the injectable pump power kept increasing, which in turn boosted the total output power of the laser. Contrary to structure with low-brightness pump sources, when utilizing a higher brightness pump source, the use of a higher brightness pump source led to an improvement in Raman conversion efficiency as the injectable pump power was increased, resulting in a steady climb in signal power. Upon reducing the fiber length to 16m, the maximum injectable pump power reached 3360W, resulting in a maximum output power of 2961W, which included a signal power of 2100W and a remaining pump power of 861W, corresponding to a Raman conversion efficiency of 62.5%. The experimental results indicate that in Raman amplifiers based on large-core graded-index fibers, augmenting pump brightness is conducive to improving conversion efficiency. Moreover, as the fiber length is shortened, the threshold for second-order Raman scattering continuously rises. Therefore, when pumping with higher brightness lasers, the signal output power can be increased by shortening the fiber length to suppress second-order

https://doi.org/10.1017/hpl.2025.29 Published online by Cambridge University Press

Raman scattering.

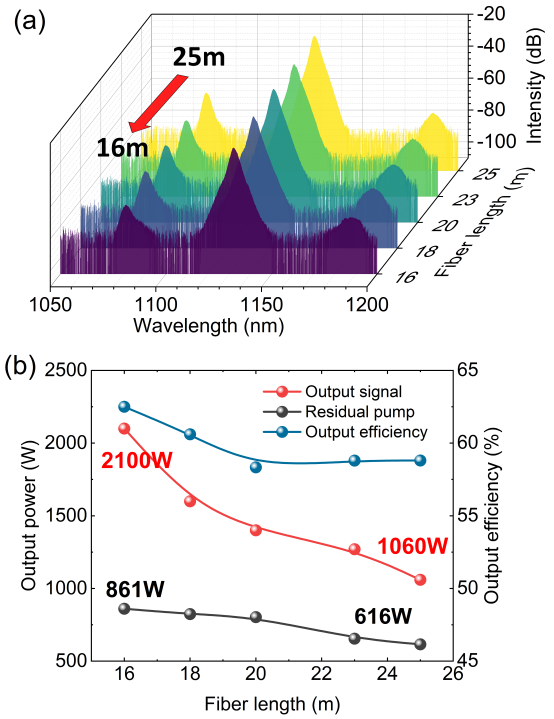

Figure 3. The maximum achievable output power at different fiber lengths with corresponding output spectrum of the Raman fiber amplifier pumped by lower brightness laser. (a) Output spectra power under maximum power at various fiber length; (b) The evolution of output power and efficiency.

3.3. Simulation of Raman fiber amplifier

To further clarify the influence of pump brightness on laser performance, we conducted simulations of the Raman conversion process within the amplifier. In the context of Raman fiber amplifiers, the power evolution can be intricately described by a set of equations that capture the dynamics of pump depletion and signal gain. The corresponding power evolution equation, which encapsulates the essence of the Raman amplification process, can be expressed as follows:

$$\Delta\Gamma_p(z) = -\frac{\omega_s}{\omega_p}\Gamma_p(z)\Delta z\frac{g_R(\omega_p,\omega_s)\Gamma_s(z)}{\Theta_{eff}(\omega_p,\omega_s)} - \alpha_p\Gamma_p(z)\Delta z \tag{1}$$

$$\Delta\Gamma_s(z) = -\frac{\omega_r}{\omega_s}\Gamma_s(z)\Delta z\frac{g_R(\omega_s,\omega_r)\Gamma_r(z)}{\Theta_{eff}(\omega_s,\omega_r)} + \Gamma_s(z)\Delta z\frac{g_R(\omega_p,\omega_s)\Gamma_p(z)}{\Theta_{eff}(\omega_p,\omega_s)} - \alpha_s\Gamma_s(z)\Delta z \tag{2}$$

$$\Delta\Gamma_r(z) = \Gamma_r(z)\Delta z\frac{g_R(\omega_s,\omega_r)\Gamma_s(z)}{\Theta_{eff}(\omega_s,\omega_r)} - \alpha_r\Gamma_r(z) \tag{3}$$

where $\Delta\Gamma$ represents the variation in optical power of the pump(p), signal(s), and 2^{nd} order Raman light(r). And g, α is the gain and loss of the mode. The effective area is correlated with the intensity distribution of the two laser components involved in Raman coupling, expressed as:

$$\Theta_{eff} = \frac{2\pi\int\Psi_p^2\rho d\rho\int\Psi_s^2\rho d\rho}{\int\Psi_p^2\Psi_s^2\rho d\rho} \tag{4}$$

where Ψ represents the modal field distribution of the laser, and ρ denotes the radial coordinate. For ease of calculation and considering the experimental setup utilizes a core-pumping structure, when low-brightness pumping is employed, the mode field area was approximated by the core area of the fiber, as the pump light predominantly fills the core. For cases with higher pump brightness, the mode field area was scaled by a factor of 0.9 to account for the tighter confinement of the pump light within the core. In our system, the peak Raman gain coefficient g_R was set to $1\times10^{-13}m/W$, which is close to the values reported in the literature for silica-based multimode fibers[44]. The fiber losses were set to 0.002 dB/m for all wavelengths in the numerical model, based on the specifications of commercially available graded-index multimode fibers and adjusted to align with experimental results.

The brightness of the pump light, which is essentially the intensity of the light per unit area, plays a pivotal role in the SRS process within a Raman fiber amplifier. When the pump light exits the combiner, it carries a specific brightness that determines how the light interacts with the signal light within the amplifier. This interaction is crucial as it dictates the transfer of energy from the pump to the signal light, which is the foundation of the amplification process. The effective area over which this energy transfer occurs is influenced by the brightness of the pump light. As the brightness changes, so does the area where the pump and signal lights interact effectively, altering the dynamics of the SRS process and, consequently, the power evolution of the laser system. To facilitate a more precise comparison with our experimental results, we ensured that the simulation parameters closely mirrored those used in the experiments, specifically regarding seed light power, pump power, and fiber specifications. Figures 4(a) and (b) depict the power evolution of the amplifier across various fiber lengths under low and high brightness pumping conditions, respectively. Concurrently, we plotted the data points of the maximum residual pump (Max.P) power and signal power (Max.S) at the laser output for various fiber lengths and connected them with lines to facilitate comparison with previous experimental findings.

https://doi.org/10.1017/hpl.2025.29 Published online by Cambridge University Press

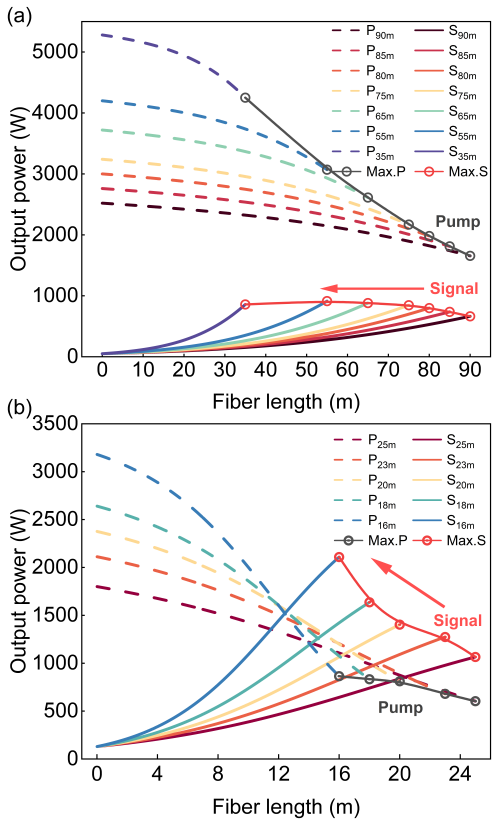

Figure 4. The output power evolution of Raman amplifier under various fiber length when pumped by lasers with different brightness (a) Result of lower brightness pumping; (b) Result of higher brightness pumping.

In Figure 4(a), it is evident that when low brightness pumping is employed, the injectable pump power increases as the fiber length is shortened. However, this increase in pump power is accompanied by a significant decline in laser efficiency, resulting in the output signal power not achieving any meaningful enhancement. This suggests that while more pump power is available, the low brightness limits the effectiveness of the stimulated Raman scattering process, ultimately constraining the overall performance of the laser. Conversely, Figure 4(b) illustrates the scenario with high brightness pumping. In this case, as the fiber length decreases, the injectable pump power not only rises but also leads to an improvement in Raman conversion efficiency. This enhancement translates into a substantial increase in the output power of the signal light. The results from our simulations align closely with the experimental data, reinforcing the validity of our modeling approach and highlighting the critical role that pump brightness plays in optimizing laser performance. Through our experiments and simulations, we can draw an initial conclusion that in Raman amplifiers based on large-core graded-index fibers, a higher pump brightness is conducive to enhancing the Raman conversion efficiency, thereby achieving a higher output power of signal light.

4. Suppression of 2^{nd} order Raman for further power scaling

In the quest to augment the power of lasers, the advent of high-order Raman emissions not only diminishes the output efficiency but also poses a grave risk to system integrity due to the backward propagation of high-order Raman light. This, in turn, constrains the potential for boosting the output power in Raman fiber lasers. To mitigate the deleterious effects of high-order Raman emissions, we have implemented a pioneering strategy: injecting an seed source at a wavelength of 1120nm with power of 130W into the amplifier through the pump arm, as illustrated in Figure 1. This extra seed induces four-wave mixing within the spectral region inhabited by high-order Raman wavelengths, thereby suppressing the rapid growth of high-order Raman light.

Figure 5(b) presents the output spectral distribution of the Raman amplifier, which incorporates an additional seed source injection. The spectrum reveals the interplay of the 1130 nm seed, 1120 nm seed, and 1080 nm pump within the fiber amplifier, giving rise to new optical frequency components via a nonlinear four-wave mixing process. These newly generated frequency components are observed at 1109 nm, 1145 nm, 1161 nm, and 1175 nm. As the power of the 1130 nm signal light increases, the second-order Raman light at 1185 nm is expected to surge rapidly upon surpassing its threshold. Nevertheless, the emergence of these new frequency components leads to a further nonlinear four-wave mixing interaction between the second-order Raman light and the components at 1161 nm and 1175 nm. This interaction results in the redistribution of power from the second-order Raman light to these new optical frequency components, thereby effectively mitigating the growth of the second-order Raman light at 1185 nm and markedly augmenting the output power of the signal light. Figure 5(c) provides a detailed representation of the Raman amplifier's output spectrum at varying output powers. It is evident that with the increment of output power, the second-order Raman light power is broadened across the 1160-1190 nm spectral band due to four-wave mixing. Concurrently, the growth in intensity of the second-order Raman light exhibits a tendency towards gradual moderation. At the peak output power, the intensity of the second-order Raman light is reduced to -30 dB relative to the signal light. Figure 5(a) depicts the evolution of the output power in relation to the injected pump power. Owing to the effective suppression of the second-order Raman light, when the pump power reaches 5.49kW, the output power of the signal light is increased to 4.08kW, with the remaining pump light at 640W, corresponding to a Raman conversion efficiency of 74.3%. Compared to using a single-wavelength seed, the output power of amplifier has doubled, the conversion efficiency has increased by 11.8%, and the second-order

https://doi.org/10.1017/hpl.2025.29 Published online by Cambridge University Press

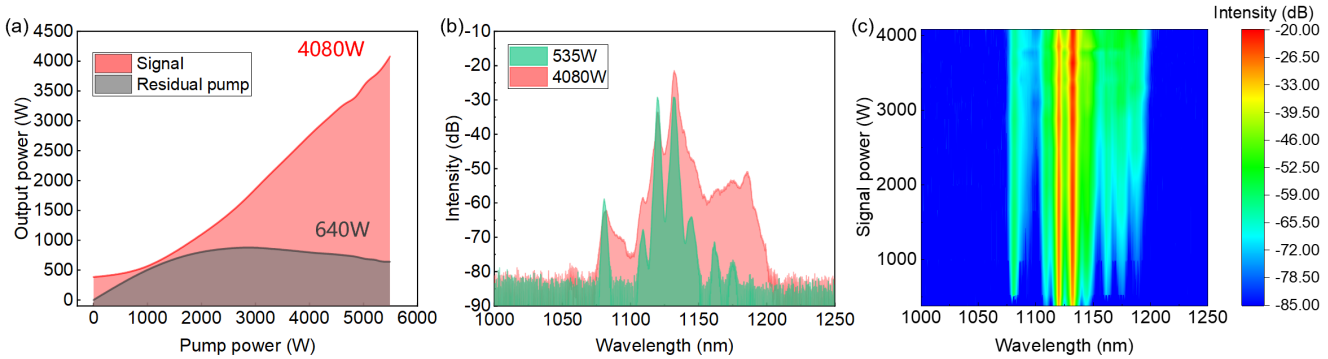

Figure 5. The output power and spectra evolution of Raman fiber amplifier with extra seed. (a) The evolution of output power; (b) Output spectra at 500W and 4kW; (c) The evolution of output spectra.

Raman effect has been significantly suppressed.

5. Conclusion

In our comprehensive study combining theoretical analysis with experimental validation, we've explored the impact of pump brightness on the output characteristics of Raman amplifiers utilizing large-core fibers. The experimental outcomes have demonstrated that insufficient pump brightness not only fails to suppress higher-order Raman effects but also significantly degrades the system's conversion efficiency. By integrating a high-brightness pump source with large-core multimodal fibers, we've effectively mitigated high-order Raman while achieving efficient stimulated Raman scattering. Building on this foundation, we've pioneered the approach of using multi-wavelength seed light to induce four-wave mixing, which has effectively curbed the rapid growth of second-order Raman light. This innovation has culminated in the realization of a 4kW Raman fiber laser output in an all-fiber structure, setting a new record for the highest reported output power to date. The methodologies and insights presented in this work offer a novel avenue for enhancing the output power of Raman fiber lasers. Moreover, this research is anticipated to have broader applications in the realms of high-power lasers, ultrafast optics, and nonlinear optics

Acknowledgement

This research was supported by National Natural Science Foundation of China (12174445, 62061136013).

References

1. C. Jauregui, J. Limpert, and A. Tünnermann, "High-power fibre lasers," *Nature Photonics*, vol. 7, no. 11, pp. 861–867, Nov. 2013. [Online]. Available: http://www.nature.com/articles/nphoton.2013.273
2. J.-h. Chen, Y.-f. Xiong, F. Xu, and Y.-q. Lu, "Silica optical fiber integrated with two-dimensional materials: towards opto-electro-mechanical technology," *Light: Science & Applications*, vol. 10, no. 1, p. 78, Apr. 2021. [Online]. Available: https://www.nature.com/articles/s41377-021-00520-x
3. J. Zuo and X. Lin, "High-power laser systems," *LASER & PHOTONICS REVIEWS*, vol. 16, no. 5, p. 2100741, May 2022. [Online]. Available: https://webofscience.clarivate.cn/wos/alldb/full-record/WOS:000765062100001
4. Y. Kawahito, H. Wang, S. Katayama, and D. Sumimori, "Ultra high power (100 kw) fiber laser welding of steel," *Optics Letters*, vol. 43, no. 19, pp. 4667–4670, Oct. 2018. [Online]. Available: https://opg.optica.org/ol/abstract.cfm?uri=ol-43-19-4667
5. D. Lee, J. Cho, C. H. Kim, and S. H. Lee, "Application of laser spot cutting on spring contact probe for semiconductor package inspection," *Optics & Laser Technology*, vol. 97, pp. 90–96, Dec. 2017. [Online]. Available: https://www.sciencedirect.com/science/article/pii/S0030399216306983
6. T. A. La, O. Ülgen, R. Shnaiderman, and V. Ntziachristos, "Bragg grating etalon-based optical fiber for ultrasound and optoacoustic detection," *Nature Communications*, vol. 15, no. 1, p. 7521, Aug. 2024. [Online]. Available: https://www.nature.com/articles/s41467-024-51497-1
7. J. Sun, R. Kuschmierz, O. Katz, N. Koukourakis, and J. W. Czarske, "Lensless fiber endomicroscopy in biomedicine," *PhotoniX*, vol. 5, no. 1, p. 18, May 2024. [Online]. Available: https://photoniX.springeropen.com/articles/10.1186/s43074-024-00133-8
8. Q. Fu, I. A. Davidson, S. M. A. Mousavi, H. C. H. Mulvad, N. V. Wheeler, L. Xu, F. Poletti, and D. J. Richardson, "Hollow-core fiber: Breaking the nonlinearity limits of silica fiber in long-distance green laser pulse delivery," *LASER & PHOTONICS REVIEWS*, vol. 18, no. 4, Apr. 2024. [Online]. Available: https://webofscience.clarivate.cn/wos/alldb/full-record/WOS:001147414600001
9. A. Wang, J. Wang, L. Jiang, L. Wang, Y. Wang, L. Yan,

https://doi.org/10.1017/hpl.2025.29 Published online by Cambridge University Press

and Y. Qin, "Experimental demonstration of 8190-km long-haul semiconductor-laser chaos synchronization induced by digital optical communication signal," *Light: Science & Applications*, vol. 14, no. 1, p. 40, Jan. 2025. [Online]. Available: https://www.nature.com/articles/s41377-024-01702-z

10. Q. Yu, Z. Yao, J. Zhou, W. Yu, C. Zhuang, Y. Qi, and H. Xiong, "Transient stimulated raman scattering spectroscopy and imaging," *Light: Science & Applications*, vol. 13, no. 1, p. 70, Mar. 2024. [Online]. Available: https://www.nature.com/articles/s41377-024-01412-6
11. Y. Dai, K. Jia, G. Zhu, H. Li, Y. Fei, Y. Guo, H. Yuan, H. Wang, X. Jia, Q. Zhao, L. Kang, J. Chen, S.-n. Zhu, P. Wu, Z. Xie, and L. Zhang, "All-fiber device for single-photon detection," *PhotoniX*, vol. 4, no. 1, p. 7, Feb. 2023. [Online]. Available: https://photoniX.springeropen.com/articles/10.1186/s43074-023-00085-5
12. M. N. Zervas and C. A. Codemard, "High power fiber lasers: A review," *IEEE Journal of Selected Topics in Quantum Electronics*, vol. 20, no. 5, pp. 219–241, Sep. 2014. [Online]. Available: https://ieeexplore.ieee.org/document/6808413
13. M. T. Sohail, J. Yin, M. Abdullah, M. Younis, M. N. Anjum, M. T. Sohail, R. Alroobaea, I. Ahmad, and Y. Peiguang, "Recent progress on high-power 2μm fiber lasers: A comprehensive study of advancements, applications, and future perspectives," *Materials Today Physics*, vol. 49, p. 101600, Dec. 2024. [Online]. Available: https://www.sciencedirect.com/science/article/pii/S2542529324002761
14. V. Dominic, S. MacCormack, R. Waarts, S. Sanders, S. Bicknese, R. Doble, E. Wolak, P. S. Yeh, and E. Zucker, "110 w fiber laser," in *Conference on Lasers and Electro-Optics (1999), paper CPD11*. Optica Publishing Group, May 1999, p. CPD11. [Online]. Available: https://opg.optica.org/abstract.cfm?uri=CLEO-1999-CPD11
15. Y. Jeong, J. K. Sahu, D. N. Payne, and J. Nilsson, "Ytterbium-doped large-core fiber laser with 1.36 kw continuous-wave output power," *Optics Express*, vol. 12, no. 25, pp. 6088–6092, Dec. 2004, publisher: Optica Publishing Group. [Online]. Available: https://opg.optica.org/oe/abstract.cfm?uri=oe-12-25-6088
16. M. O'Connor, V. Gapontsev, V. Fomin, M. Abramov, and A. Ferin, "Power scaling of sm fiber lasers toward 10kw," in *Conference on Lasers and Electro-Optics/International Quantum Electronics Conference (2009), paper CThA3*. Optica Publishing Group, May 2009, p. CThA3. [Online]. Available: https://opg.optica.org/abstract.cfm?uri=CLEO-2009-CThA3
17. V. R. Supradeepa, Y. Feng, and J. W. Nicholson, "Raman fiber lasers," *Journal of Optics*, vol. 19, no. 2, p. 023001, Feb. 2017. [Online]. Available: https://iopscience.iop.org/article/10.1088/2040-8986/19/2/023001
18. T. Yao, C. Fan, X. Hao, Y. Li, S. Huang, H. Zhang, J. Xu, J. Ye, J. Leng, and P. Zhou, "Research progress in power scaling and wavelength extension of raman fiber lasers (invited)," *Chinese Journal of Lasers*, vol. 51, no. 19, p. 1901010, Oct. 2024. [Online]. Available: https://www.researching.cn/articles/OJ8084370d5e19808a
19. V. R. Supradeepa and J. W. Nicholson, "Power scaling of high-efficiency 1.5 μm cascaded raman fiber lasers," *Optics Letters*, vol. 38, no. 14, pp. 2538–2541, Jul. 2013. [Online]. Available: https://opg.optica.org/abstract.cfm?URI=ol-38-14-2538
20. H. Wu, Z. Wang, W. Sun, Q. He, Z. Wei, and Y.-J. Rao, "1.5μm low threshold, high efficiency random fiber laser with hybrid erbium–raman gain," *Journal of Lightwave Technology*, vol. 36, no. 4, pp. 844–849, Feb. 2018. [Online]. Available: https://ieeexplore.ieee.org/document/7939975/
21. V. Balaswamy, S. Aparanji, S. Arun, S. Ramachandran, and V. R. Supradeepa, "High-power, widely wavelength tunable, grating-free raman fiber laser based on filtered feedback," *Optics Letters*, vol. 44, no. 2, pp. 279–282, Jan. 2019. [Online]. Available: https://opg.optica.org/ol/abstract.cfm?uri=ol-44-2-279
22. S. Loranger, A. Tehranchi, H. Winful, and R. Kashyap, "Realization and optimization of phase-shifted distributed feedback fiber bragg grating raman lasers," *Optica*, vol. 5, no. 3, p. 295, Mar. 2018. [Online]. Available: https://opg.optica.org/abstract.cfm?URI=optica-5-3-295
23. S. A. Babin, "High-brightness all-fiber raman lasers directly pumped by multimode laser diodes," *High Power Laser Science and Engineering*, vol. 7, p. e15, 2019. [Online]. Available: https://www.cambridge.org/core/product/identifier/S2095471918000762/type/journal_article
24. P. Zheng, D. Wu, and S. Dai, "Wavelength tunable raman fiber laser based on raman gain spectrum control," *Optics & Laser Technology*, vol. 164, p. 109496, Sep. 2023. [Online]. Available: https://linkinghub.elsevier.com/retrieve/pii/S0030399223003894
25. Y. Feng, L. R. Taylor, and D. B. Calia, "150 w highly-efficient raman fiber laser," *Optics Express*, vol. 17, no. 26, pp. 23 678–23 683, Dec. 2009. [Online]. Available: https://opg.optica.org/oe/abstract.cfm?uri=oe-17-26-23678
26. H. Zhang, H. Xiao, P. Zhou, X. Wang, and X. Xu, "119-w monolithic single-mode 1173-nm raman fiber laser," *IEEE Photonics Journal*, vol. 5, no. 5, pp. 1 501 706–1 501 706, Oct. 2013. [Online]. Available: http://ieeexplore.ieee.org/document/6576180/
27. C. A. Codemard, J. Ji, J. K. Sahu, and J. Nilsson,

https://doi.org/10.1017/hpl.2025.29 Published online by Cambridge University Press

"100-w cw cladding-pumped raman fiber laser at 1120 nm," in *Fiber Lasers VII: Technology, Systems, and Applications*, vol. 7580. SPIE, Feb. 2010, pp. 444–450. [Online]. Available: https://www.spiedigitallibrary.org/conference-proceedings-of-spie/7580/75801N/100-W-CW-cladding-pumped-Raman-fiber-laser-at-1120/10.1117/12.845606.full

28. Y. Shamir, Y. Glick, M. Aviel, A. Attias, and S. Pearl, "250 w clad pumped raman all-fiber laser with brightness enhancement," *Optics Letters*, vol. 43, no. 4, pp. 711–714, Feb. 2018. [Online]. Available: https://opg.optica.org/abstract.cfm?URI=ol-43-4-711
29. Y. Glick, Y. Shamir, M. Aviel, Y. Sintov, S. Goldring, N. Shafir, and S. Pearl, "1.2 kw clad pumped raman all-passive-fiber laser with brightness enhancement," *Optics Letters*, vol. 43, no. 19, pp. 4755–4758, Oct. 2018. [Online]. Available: https://opg.optica.org/abstract.cfm?URI=ol-43-19-4755
30. Y. Glick, V. Fromzel, J. Zhang, A. Dahan, N. Ter-Gabrielyan, R. K. Pattnaik, and M. Dubinskii, "High power, high efficiency diode pumped raman fiber laser," *Laser Physics Letters*, vol. 13, no. 6, p. 065101, Jun. 2016. [Online]. Available: https://iopscience.iop.org/article/10.1088/1612-2011/13/6/065101
31. Y. Glick, V. Fromzel, J. Zhang, N. Ter-Gabrielyan, and M. Dubinskii, "High efficiency, 154 w cw, diode-pumped raman fiber laser with brightness enhancement," *Applied Optics*, vol. 55, no. 3, p. B97, 2016. [Online]. Available: https://doi.org/10.1364/AO.56.000B97
32. Y. Glick, Y. Shamir, A. A. Wolf, A. V. Dostovalov, S. A. Babin, and S. Pearl, "Highly efficient all-fiber continuous-wave raman graded-index fiber laser pumped by a fiber laser," *Optics Letters*, vol. 43, no. 5, pp. 1027–1030, Mar. 2018. [Online]. Available: https://opg.optica.org/abstract.cfm?URI=ol-43-5-1027
33. E. A. Evmenova, S. I. Kablukov, I. N. Nemov, A. A. Wolf, A. V. Dostovalov, V. A. Tyrtyshnyy, D. V. Myasnikov, and S. A. Babin, "High-efficiency ld-pumped all-fiber raman laser based on a 100 μm core graded-index fiber," *Laser Physics Letters*, vol. 15, no. 9, p. 095101, Sep. 2018. [Online]. Available: https://iopscience.iop.org/article/10.1088/1612-202X/aacca7
34. C. Fan, M. Fu, X. Hao, S. Huang, Y. Li, Z. Chen, J. Leng, T. Yao, and P. Zhou, "All-fiber raman oscillator with 1.8 kw output power," *Infrared and Laser Engineering*, vol. 53, no. 5, p. 20240031, 2024. [Online]. Available: https://www.researching.cn/articles/OJ2de3d0fa7be51c04
35. Y. Chen, J. Leng, H. Xiao, T. Yao, J. Xu, and P. Zhou, "High-efficiency all-fiber raman fiber amplifier with record output power," *Laser Physics Letters*, vol. 15, no. 8, p. 085104, Aug. 2018. [Online]. Available: https://iopscience.iop.org/article/10.1088/1612-202X/aac428
36. Y. Chen, T. Yao, H. Xiao, J. Leng, and P. Zhou, "Greater than 2 kw all-passive fiber raman amplifier with good beam quality," *High Power Laser Science and Engineering*, vol. 8, p. e33, 2020. [Online]. Available: https://www.cambridge.org/core/product/identifier/S209547192000033X/type/journal_article
37. Y. Chen, J. Leng, H. Xiao, T. Yao, and P. Zhou, "Pure passive fiber enabled highly efficient raman fiber amplifier with record kilowatt power," *IEEE Access*, vol. 7, pp. 28 334–28 339, 2019. [Online]. Available: https://ieeexplore.ieee.org/document/8642309/
38. Y. Chen, T. Yao, H. Xiao, J. Leng, and P. Zhou, "3 kw passive-gain-enabled metalized raman fiber amplifier with brightness enhancement," *Journal of Lightwave Technology*, vol. 39, no. 6, pp. 1785–1790, Mar. 2021. [Online]. Available: https://ieeexplore.ieee.org/document/9265192
39. C. Fan, H. Xiao, T. Yao, J. Xu, Y. Chen, J. Leng, and P. Zhou, "Kilowatt level raman amplifier based on 100 μm core diameter multimode grin fiber with m2 = 1.6," *Optics Letters*, vol. 46, no. 14, p. 3432, Jul. 2021. [Online]. Available: https://opg.optica.org/abstract.cfm?URI=ol-46-14-3432
40. C. Fan, Y. Li, X. Hao, T. Yao, J. Leng, and P. Zhou, "Strategic modal management for enhanced stimulated raman scattering in optical fibers," *Optics Express*, vol. 32, no. 25, pp. 44 186–44 198, Dec. 2024. [Online]. Available: https://opg.optica.org/oe/abstract.cfm?uri=oe-32-25-44186
41. K. Krupa, A. Tonello, B. M. Shalaby, M. Fabert, A. Barthélémy, G. Millot, S. Wabnitz, and V. Couderc, "Spatial beam self-cleaning in multimode fibres," *Nature Photonics*, vol. 11, no. 4, pp. 237–241, Apr. 2017. [Online]. Available: https://www.nature.com/articles/nphoton.2017.32
42. N. B. Terry, T. G. Alley, and T. H. Russell, "An explanation of SRS beam cleanup in graded-index fibers and the absence of SRS beam cleanup in step-index fibers," *Optics Express*, vol. 15, no. 26, pp. 17 509–17 519, Dec. 2007. [Online]. Available: https://opg.optica.org/abstract.cfm?URI=oe-15-26-17509
43. Y. Chen, J. Song, J. Ye, T. Yao, J. Xu, H. Xiao, J. Leng, and P. Zhou, "Power scaling of raman fiber amplifier based on the optimization of temporal and spectral characteristics," *Optics Express*, vol. 28, no. 8, p. 12395, Apr. 2020. [Online]. Available: https://opg.optica.org/abstract.cfm?URI=oe-28-8-12395
44. A. Polley and S. E. Ralph, "Raman Amplification in Multimode Fiber," *IEEE Photonics Technology Letters*, vol. 19, no. 4, pp. 218–220, 2007. [Online]. Available: http://ieeexplore.ieee.org/document/4077082/

https://doi.org/10.1017/hpl.2025.29 Published online by Cambridge University Press